Status of Hadron Spectroscopy at LEAR

Curtis A. Meyer

Carnegie Mellon University, Pittsburgh, PA 15217

Abstract

Recent observations by the Crystal Barrel experiment of two scalar resonances, $f_0(1370)$ and $a_0(1450)$ have allowed us to clarify the members of the scalar nonet. In addition, a third scalar, $f_0(1500)$, appears to be supernumerary, and is a candidate for the scalar glueball expected near 1550 MeV.

Light Quark Meson Spectroscopy

Light quark meson spectroscopy studies the mesons which are made up of u, d, and s quarks. Within the quark model, these mesons come in nonets of definite spin, parity and C–parity, J^{PC}, where these quantum numbers are produced by the relative state of the quark–antiquark pair. The spin $\frac{1}{2}$ quarks and antiquarks can combine into either a spin singlet, $S = 0$ state, or a spin triplet, $S = 1$ state. In addition, there can be a relative orbital angular momentum L between the quark and the antiquark, $L = 0, 1, 2, \cdots$. Finally, the $q\bar{q}$ system can have radial excitations where the principal quantum number N takes on values $1, 2, \cdots$. The total angular momentum J is then formed by combining L and S. Using these quantum numbers, we can describe a given nonet via spectroscopic notation as $N^{2S+1}L_J$, or in terms of the conserved quantum numbers of the strong interaction $I^G J^{PC}$. Where the system has isospin I, G–parity, $G = (-1)^{L+S+I}$, total spin J, parity $P = -(-1)^L$ and C–parity, $C = (-1)^{L+S}$.

Fig. 1 shows the known light–quark mesons classified in this manner, as well as a few additional states which do not seem to fit into the scheme. It is actually the states which do not fit into the $q\bar{q}$ classification, the so called *exotics*, which are the main interest in light quark meson spectroscopy. These exotics include *glueballs*, bound states of gluons, *hybrid mesons*, meson states containing a valance gluon, and so called 4–quark states, $q\bar{q}q\bar{q}$, all of which are predicted by models of low energy QCD. There are several tools available to identify these states:

- Quantum Numbers, $(I^G)J^{PC}$ identify if the state can be assigned to a nonet, or if the nonet is full, they identify the state as supernumerary.

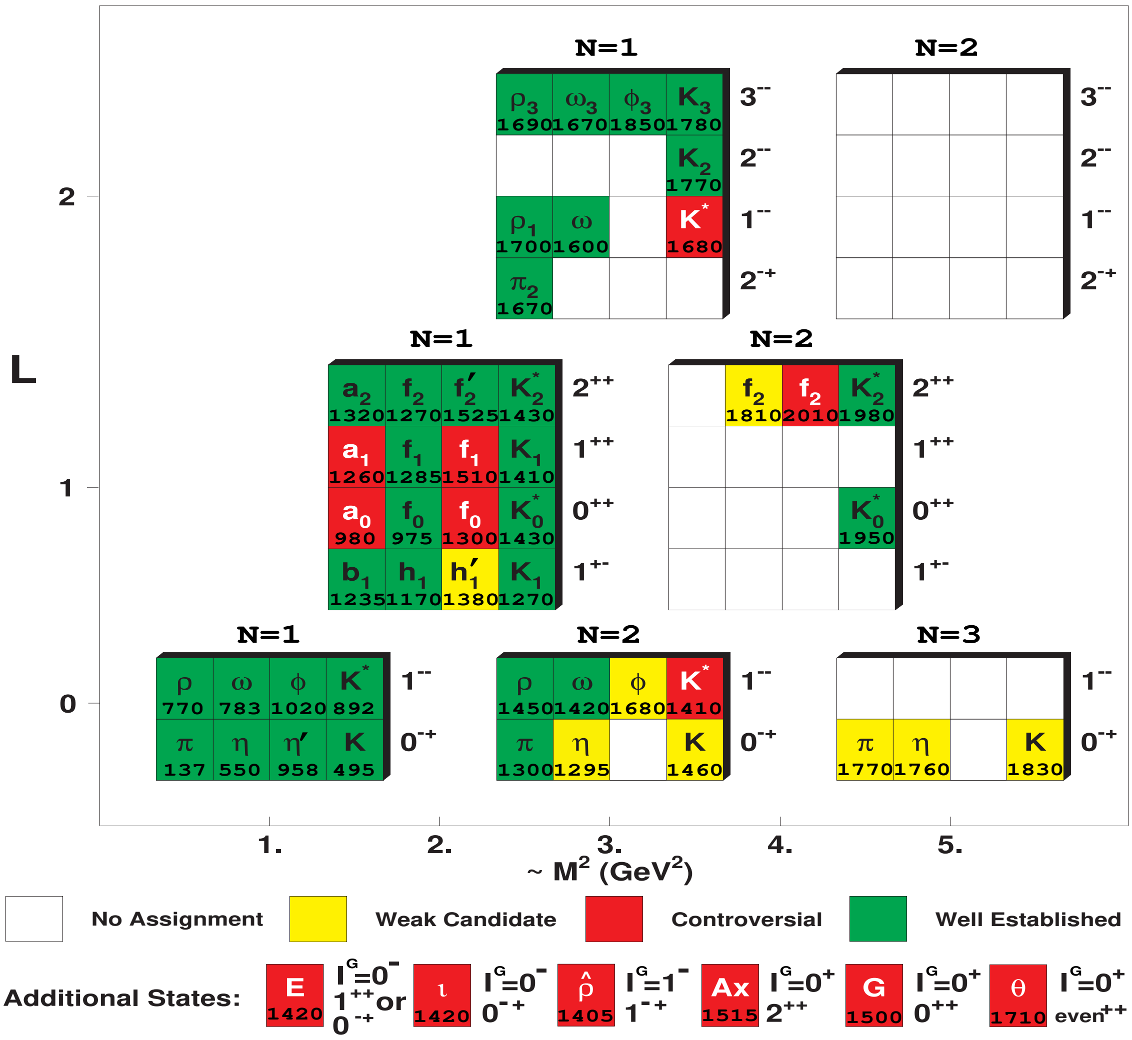

Figure 1: The expected spectrum of light–quark mesons.

- Decay patterns, $\mathrm{B}r(x \to ab)$: $\mathrm{B}r(x \to cd)$: $\cdots$ measure the quark content of the state. In particular the mixing of $\bar{u}u$, $\bar{d}d$ and $\bar{s}s$.
- Production Mechanisms, particularly gluon rich mechanisms provide likely hunting grounds for exotics.
  - Radiative J/Ψ decay, (gluon rich) — $J/\Psi \to \gamma x$
  - Proton antiproton annihilation, (gluon rich) — $\bar{p}p \to xa$
  - Central Production (gluon rich) — $pp \to p_f x p_s$.
  - Photoproduction, (gluon poor) — $\gamma p \to xp$
  - Two Photon Production (gluon poor) —$\gamma\gamma \to x$

As an example of an exotic state, consider the *glueball* – a bound state of 2 or 3 gluons. In most models, the ground state glueball is expected to be a scalar object, $I = 0$, $J^{PC} = 0^{++}$. In addition, lattice calculations, and the fluxtube model both predict that the ground state glueball should have a mass of 1500 to 1600 MeV/c^2. Unfortunately, these are exactly the quantum numbers of the scalar mesons, f_0 and f_0'. The mass is also more or less where one would expect to find the scalar mesons. In this case, the quantum numbers alone will be insufficient to identify the glueball. However, we can also examine the decay pattern of a glueball. Assuming flavor democracy, or equal coupling to u, d and s quarks, one would expect the following decay patterns:

$$\pi\pi : \eta\eta : \eta\eta' : K\bar{K} = 3 : 1 : 0 : 4 \tag{1}$$

For production, one would expect to see the glueball in the gluon–rich production mechanisms: radiative J/Ψ, $\bar{p}p$ annihilation, and central production, while one would expect this to not be present in channels like photoproduction, and $\gamma\gamma$. Finally, if the glueball were to lie near in mass to mesons of the same quantum numbers, one would not be surprised to see mixing of these states, which could distort the decay pattern.

The Analysis Method

Most of the results presented here come from the Crystal Barrel Detector at LEAR, [1] a nearly 4π apparatus for both charged particles and photons. The detector is used to study $\bar{p}p$ annihilation at rest and in flight, (up to 1.9GeV/c), and has been very productive in the field of meson spectroscopy. The detector is shown in Fig. 2. The antiprotons enter along the axis of the 1.5 T solenoidal field, and stop in a liquid hydrogen target. They annihilate, and the resulting $\pi^\pm$, $K^\pm$ and γ's are tracked outward through the detector.

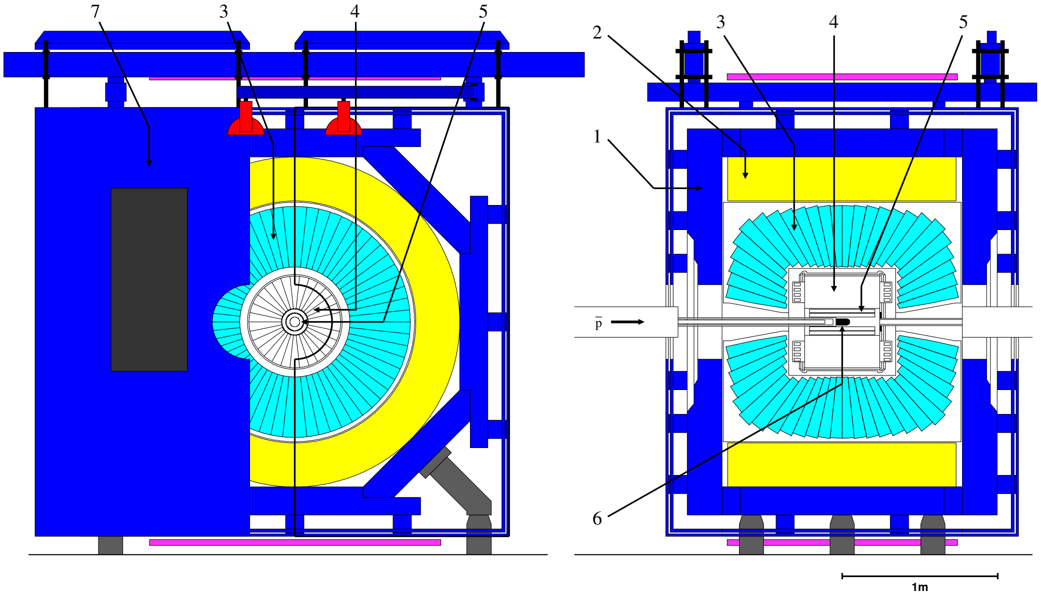

Figure 2: The Crystal Barrel detector. Magnet yoke (1), magnet coils (2), CsI–calorimeter (3), JDC (4), PWC (5), target (6), one half of the endplate (7).

Immediately outside the hydrogen target are two cylindrical multiwire proportional chambers used to either trigger on or veto events with charged particles. Next is a 23 layer cylindrical drift chamber, (JDC). The chamber is divided axially into 30 sectors, with an 8mm wire spacing between adjacent radial layers. The wires are read out at each end to provide a z–measurement through charge division. Outside the JDC is the CsI(Tl) barrel built from 1380 16 radiation length crystals. The crystals are arranged in a center–pointing geometry, and the calorimeter has achieved an energy resolution of 2.5% at 1GeV.

The data presented here arise from $\bar{p}p$ annihilations at rest. For annihilations in a liquid hydrogen target, it is known that most of the $\bar{p}p$ atoms annihilate from an initial S-state, $^1S_0$ or $^3S_1$. In this situation, the quantum numbers of the the initial state are known as 0^{-+} an 1^{--} respectively. These data are analyzed within the framework of the isobar model. Assuming that we have three mesons in the final state, a, b and c, then the transition from the initial to final state is assumed to proceed through a series of quasi two–body intermediate states, A, B and C. The decay momentum $\vec{p}$ describes the two particles from the initial $\bar{p}p$ system, while the decay momentum $\vec{q}$ is measured in the rest frame of the intermediate two–body state. As an example, the following processes might be possible.

$$\begin{array}{lll} \overbrace{\bar{p}p}^{J^{PC}} \rightarrow & \overbrace{Ac}^{L,\vec{p}} \rightarrow & \overbrace{(ab)}^{l,\vec{q}}\,c \\ \bar{p}p \rightarrow & aB \rightarrow & a(bc) \\ \bar{p}p \rightarrow & bC \rightarrow & b(ac) \end{array}$$

The transition amplitude $\mathcal{A}$ can be written for a particular partial wave as:

$$\mathcal{A}_{J^{PC}}(\vec{p},\vec{q}) = \sum_{sym} \underbrace{Z_{J^{PC},l,L}(\vec{p},\vec{q})}_{spin-parity\,fcn.} \overbrace{D_L(\vec{p})}^{barrier\,fcn.} \underbrace{F_l(\vec{q})}_{dynamical\,fcn.} \tag{2}$$

where Z is a spin–parity function, D is a centrifugal barrier function, and F is a dynamical function. In the case of a single resonance, F would be written as a Breit–Wigner function. However, in the case of the scalar meson sector, where one has many broad, overlapping resonances, a more detailed parametrization of F is needed. In this case, the K–matrix approach is used to describe the decay of a resonance into several different final states [2]. The real, symmetric K–matrix can be written as:

$$K_{ij} = \sum_{alpha} \frac{g_{\alpha i} g_{\alpha j} D^l_{\alpha i}(q,q_\alpha) D^l_{\alpha j}(q,q_\alpha)}{m_\alpha^2 - m^2} + c_{ij}$$

where m_α are the K–matrix poles, $g_{\alpha i}$ describes the coupling of the α'th pole to the i'th decay channel, $D^l_{\alpha i}(q,q_\alpha)$ is a centrifugal barrier term and c_{ij} is a real background constant. The coupling g can itself be written as

$$g_{\alpha i} = \sqrt{\frac{m_\alpha \Gamma_{\alpha i}}{\rho_i(m_\alpha)}}$$

where $\Gamma_{\alpha i}$ is the partial decay width, and ρ_i describes the two–body phase space, $\rho_i = \frac{2q_i}{m_i}$. The T–matrix can then be written in terms of the K–matrix as:

$$T = (1 - iK\rho)^{-1} K.$$

It is then the poles of the T–matrix which describe the resonance parameters. In addition, the production is described using the P–vector approximation of Aitchison.

$$P_i = \sum \frac{\beta_\alpha g_{\alpha i}}{m_{\alpha^2} - m^2},$$

which then leads to the F–vector,

$$\vec{F} = (1 - iK\rho)^{-1} \vec{P} \tag{3}$$

This parametrization for F is used in equation 2 to fit the data, and extract the resonance parameters.

The Scalar Mesons

The first three data sets discussed in this paper come from an all–neutral trigger, (no charged particles in the PWC). The 6γ final state is obtained from $16.8 \cdot 10^6$ all neutral annihilations at rest, where we reconstruct $\bar{p}p \rightarrow \pi^\circ\pi^\circ\pi^\circ$ (712k events), $\bar{p}p \rightarrow \pi^\circ\pi^\circ\eta$ (374k events) and $\bar{p}p \rightarrow \pi^\circ\eta\eta$ (198k events) where π° and η are detected in their 2γ decay modes. These three data sets have been analyzed using a coupled channel technique in the K–matrix formalism. This formalism allows for example a $\pi^\circ\pi^\circ$ resonance to be observed in both the $\pi^\circ\pi^\circ\pi^\circ$ and $\pi^\circ\pi^\circ\eta$ final states. The same decays are involved in both, but a different production mechanism is allowed. In addition, a resonance decaying to both $\pi^\circ\pi^\circ$ and $\eta\eta$ could be observed via the same production mechanism in both $\pi^\circ\pi^\circ\pi^\circ$ and $\pi^\circ\eta\eta$, but a different decay is involved in each. A very important element of these analysis is the correct treatment of the isospin 0, $\pi\pi$ S–wave scattering which we refer to as σ. We have taken the parametrization of Au, Morgan and Pennington [3], (AMP) to describe the $\pi\pi$ scattering as a function of the $\pi\pi$ invariant mass up to the $f_0(980)$. This must then smoothly connect to our solution for higher $\pi\pi$ masses. The following summarizes the results in this analysis.

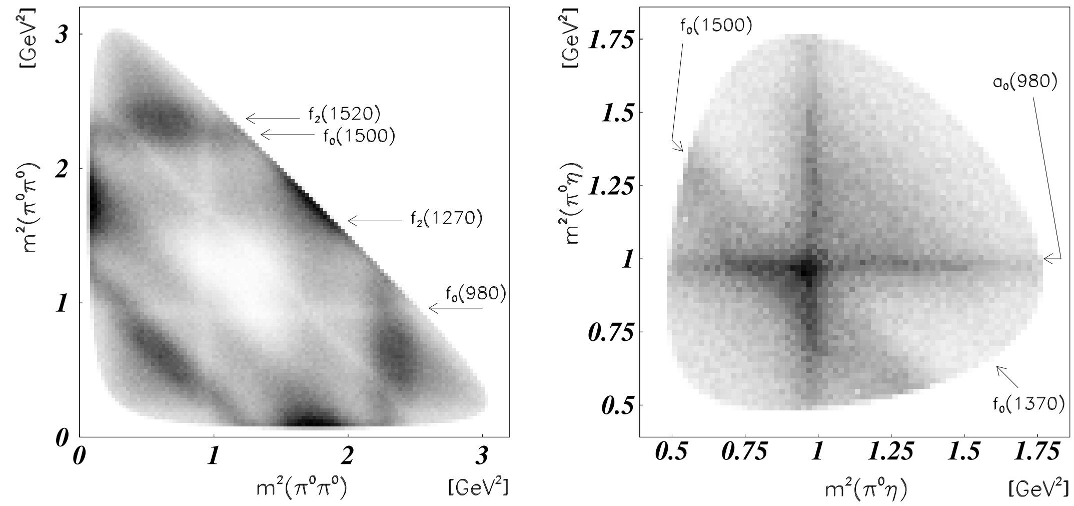

Figure 3: The Dalitz plots for $\bar{p}p \rightarrow \pi^\circ\pi^\circ\pi^\circ$ (left) and $\eta\eta\pi^\circ$ (right).

The $\bar{p}p \rightarrow \pi^\circ\pi^\circ\pi^\circ$ Dalitz plot (Fig. 3–left) has 3–fold symmetry, meaning that resonances are seen simultaneously as three bands, vertical, horizontal and diagonal. In the vertical, one sees a band near 0.9 GeV^2 corresponding to the $f_0(980)$. The two blobs at the upper and lower edge of the plot near 1.7 GeV^2 corresponds to the $f_2(1270)$, and the vertical band near 2.25 GeV^2 corresponds to a new scalar resonance, the $f_0(1500)$. The blob near 2.4 GeV^2 is caused by reflections from the low–mass $\pi\pi$ S–wave system, and a tensor state, ($J^{PC} = 2^{++}$) near 1550 MeV. In addition, the fit to this Dalitz plot requires a broad, inelastic scalar state at a mass of 1370 MeV, which is probably the $f_0(1300)$. There is a very broad background pole at a mass 1000 MeV/c^2. The mass and width of this latter pole tend to move around. [4],[5],[6]

The $\eta\eta\pi^\circ$ Dalitz plot (Fig. 3–right) has a 2–fold symmetry. Resonances in the $\eta\pi^\circ$ system are seen as horizontal and vertical bands, while resonances in the $\eta\eta$ system are seen as diagonal bands. The Dalitz plot shows a clear signal for the $a_0(980) \to \eta\pi^\circ$ as the horizontal and vertical crossing bands near 0.96 GeV^2. In addition, there are two diagonal bands corresponding to the $f_0(1370) \to \eta\eta$ and the $f_0(1500) \to \eta\eta$. [4],[7],[8]

The Dalitz plot for $\bar{p}p \to \eta\pi^\circ\pi^\circ$ (Fig. 4–left), exhibits a very complicated interference pattern which is evidence for dominance of a single initial state. The $\eta\pi^\circ\pi^\circ$ final state arises almost entirely from the $^1S_0$ state of the $\bar{p}p$ atom. The analysis explains the data using the following amplitudes. [$\pi\pi$ S–wave]

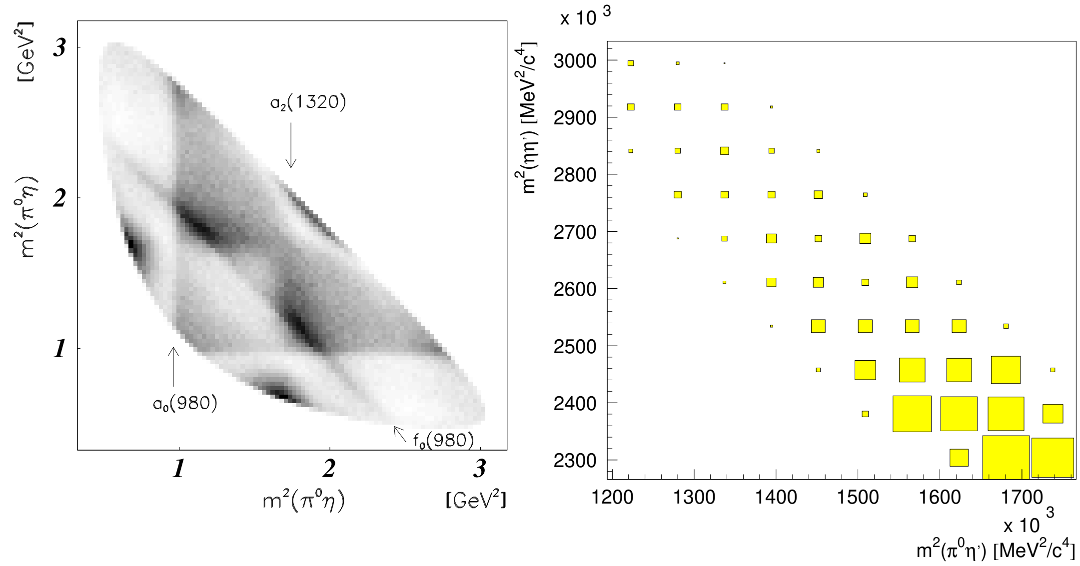

Figure 4: The Dalitz plots for $\bar{p}p \to \pi^\circ\pi^\circ\eta$ (left) and $\eta'\eta\pi^\circ$ (right).

Including the AMP parametrization [3], $f_0(980)$ and $f_0(1370)$ explain 50 to 55% of the data. [$\pi\eta$ S–wave] The $a_0(980)$ explains 13 to 15% of the data. In addition the data demand a second resonance, the $a_0(1450)$, $m = (1470 \pm 25)$, $\Gamma = (265 \pm 30)$, which explains 5% of the data. Ignoring the second resonance causes the χ^2/N_{dof} to increase from 1.2 to 2.5 [9]. [$\pi\eta$ P–wave] A broad non–resonant background wave is needed to explain about 1.5 to 4.5% of the data. We exclude a resonance interpretation with the mass and width reported by GAMS for the $\hat{\rho}(1405)$ [10]. [$\eta\pi$ d–wave] The $a_2(1320)$ describes 18 to 28% of the data. In addition, a second a_2 is needed to account for about 2% of the data. However, its mass is at the edge of phase space, and we do not claim that this is a resonance. [4]

A simultaneous spin–parity analysis [4] of $\pi^\circ\pi^\circ\pi^\circ$, $\eta\pi^\circ\pi^\circ$ and $\eta\eta\pi^\circ$ yields the following parameters for the two isoscalar scalar resonances and the new isovector scalar resonance:

$$\begin{array}{lll} f_0(1370) & m = 1390 \pm 30 & \Gamma = 390 \pm 80 \\ f_0(1500) & m = 1500 \pm 10 & \Gamma = 154 \pm 30 \\ a_0(1450) & m = 1470 \pm 25 & \Gamma = 265 \pm 30 \end{array}$$

and the product branching ratios for $f_0(1500)$ are measured to be:

$$\begin{aligned} \mathrm{B}R(\bar{p}p \to f_0(1500)\pi^\circ, f_0(1500) \to \pi^\circ\pi^\circ) &= (1.27 \pm 0.33) \cdot 10^{-3} \\ \mathrm{B}R(\bar{p}p \to f_0(1500)\pi^\circ, f_0(1500) \to \eta\eta) &= (0.60 \pm 0.17) \cdot 10^{-3}. \end{aligned}$$

In addition to the previous three final states, an independent spin–parity analysis of $\bar{p}p \to \eta'\eta\pi^\circ$ has been made using 977 $\eta'\eta\pi^\circ$ events reconstructed from the 6γ final state [11]. The Dalitz plot from these events is shown in Fig. 4–right. The enhancement in the lower right corner of the Dalitz plot is identified as a $J^{PC} = 0^{++}$ object in the $\eta'\eta$ system. This isospin 0 object is identified as the $f_0(1500)$ decaying into $\eta'\eta$. We measure its mass, width and branching fraction to be:

$$m = (1545 \pm 25) \quad \Gamma = (100 \pm 40)$$

$$\mathrm{B}R(\bar{p}p \to f_0(1500)\pi^\circ, f_0(1500) \to \eta'\eta) = (1.70 \pm 0.40) \cdot 10^{-4}.$$

A second analysis of these data using a mass independent width to fit the f_0 finds an equally good solution with a mass of 1500 MeV/c^2 and a width of 120 MeV/c^2. This solution has a branching ratio that is 20% higher than quoted above.

The $K\bar{K}\pi^\circ$ final state is very important in classifying mesons. In Fig. 5–left is shown a very preliminary Dalitz plot for the $K_L K_L \pi^\circ$ final state. The $K^*(890)$ can be seen as crossing horizontal and vertical bands near 0.8 GeV^2. In addition, there are at least three diagonal bands ($K_L K_L$ resonances). Preliminary results from the spin parity analysis need the $f_0(1500)$ decaying into $K_L K_L$. However at present, we only find an upper limit which is consistent with an older bubble chamber limit [12] of

$$\mathrm{B}R(\bar{p}p \to f_0(1500)\pi^\circ, f_0(1500) \to K_L K_L) < (3.6) \cdot 10^{-4}.$$

The system $\bar{p}p \to \pi^+\pi^-\pi^\circ\pi^\circ\pi^\circ$ has been examined to search for resonances decaying into $\rho^+\rho^-$ [13]. The mass–mass plot, (Fig. 5–right) shows an enhancement in the $\rho^+\rho^-$ data over the background. The analysis of these data show the presence of a scalar resonance X decaying into $\rho\rho$ and $\sigma\sigma$, where σ is the $\pi\pi$ S–wave. We find $m_X = 1374 \pm 38$ MeV and $\Gamma_X = 375 \pm 61$ MeV. Under the assumption that this is isoscalar, it is probably the inelastic $f_0(1370)$ seen above, and we estimate that its 4π:2π decay ratio is approximately 5:1.

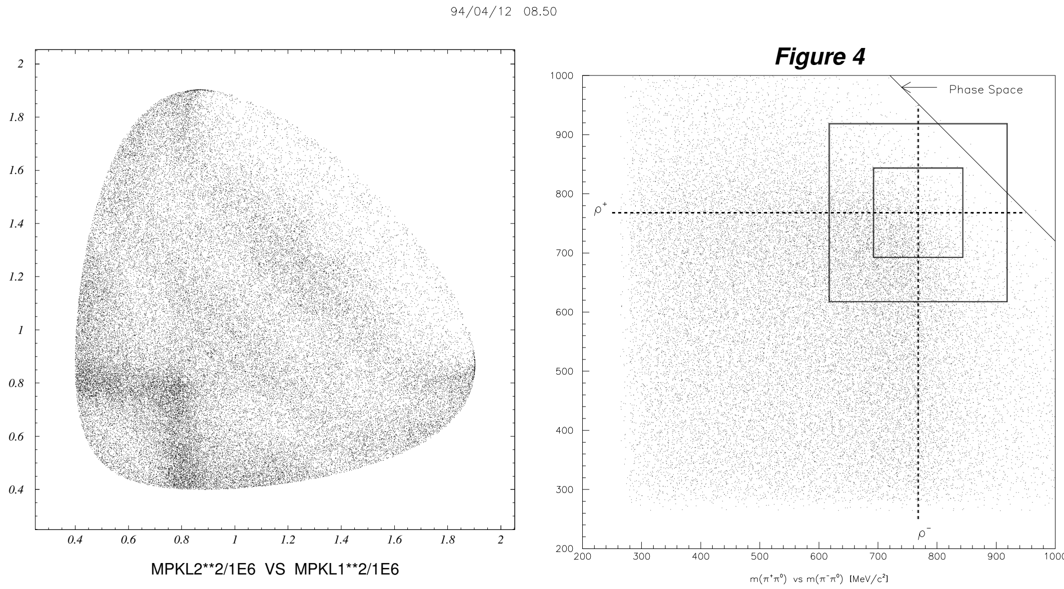

Figure 5: The Dalitz plots for $\bar{p}p \rightarrow \pi^{\circ} K_L K_L$ (left) and the mass–mass plot from $\pi^{+}\pi^{-}\pi^{\circ}\pi^{\circ}\pi^{\circ}$.

The Scalar Nonet

In Table 1 are shown the ground state $L = 1$ nonets in the quark model as assigned by the Particle Data Group [14]. Normally, the octet and singlet $I = 0$ members of the nonets are mixed. In the case of an ideally mixed nonet, (complete separation between the $u\bar{u} + d\bar{d}$ and the $s\bar{s}$ components), $\Theta = 35.3^{\circ}$. In table 1 are given the two mixing angles for the PDG assignments for all except the scalars. Most of these are fairly close to ideally mixed.

Looking at the 0^{++} assignment, it is fairly clear that the $a_0(980)$ and the $f_0(980)$ do not fit well into the nonet. Other evidence from both two–photon couplings and J/ψ decays indicate that these states are not simple $q\bar{q}$ systems. If these are not members of the scalar nonet, what are the members? The $f_0(1370)$, (probably the $f_0(1300)$), is a good candidate for the lightest $I = 0$ member. In addition the $a_0(1450)$ fits naturally in as the $I = 1$ member. Using the mass of the $K_0^*(1430)$, we can compute a scalar nonet mixing angle of either 62° or 118°. The question then arises as to where is the f_0'? There are several additional 0^{++} states that could possibly be this state. The $f_0(1500)$ from Crystal Barrel, the $f_0(1520)$ from LASS [15], the $f_0(1590)$ or G–meson from GAMS [16], and possibly the $f_J(1710)$ or Θ. Using the mixing angle for the scalar nonet, we would expect the f_0' to have a mass of 1500–1800 MeV and relative decay widths as given in table 2. Correcting the measured branching fractions for the $f_0(1500)$ by its decay momentum yields the relative decay strengths given in the $f_0(1500)$ row of table 2. The most obvious conclusion

$^{2S+1}L_J$ J^{PC}	$I=1$ $u\bar{d}$, $u\bar{u}$, $d\bar{d}$	$I=0$ $u\bar{u}$, $d\bar{d}$,		$I=0$ $s\bar{s}$		$I=1/2$ $\bar{s}u$, $\bar{s}d$	Θ
$^1P_1$	$b_1(1235)$	$h_1(1170)$,		$h_1'(1380)$		$K_1(1270)$	41°
1^{+-}	$\Gamma=155$	$\Gamma=360$,		$\Gamma=80$	$K\bar{K}^*$	$K_1(1400)$	
$^3P_0$	$a_0(980)$	$f_0(975)$,		$f_0(1300)$		$K_0^*(1430)$	
0^{++}	$\Gamma=57$	$\Gamma=47$,	20% $K\bar{K}$	$\Gamma=400$	93% $\pi\pi$	$\Gamma=287$	
$^3P_1$	$a_1(1260)$	$f_1(1285)$,		$f_1(1510)$		$K_1^*(1400)$	38°
1^{++}	$\Gamma=400$	$\Gamma=25$,	$K\bar{K}^*$	$\Gamma=35$	10% $K\bar{K}$	$K_1(1270)$	
$^3P_2$	$a_2(1320)$	$f_2(1270)$,		$f_2'(1525)$		$K_2(1430)$	31°
2^{++}	$\Gamma=110$	$\Gamma=185$,	5% $K\bar{K}$	$\Gamma=85$	71% $K\bar{K}$	$\Gamma=105$	
New 0^{++} Assignment							
$^3P_0$	$a_0(1450)$	$f_0(1370)$,		$f_0'(????)$		$K_0^*(1430)$	62°
0^{++}	$\Gamma=250$	$\Gamma=267$,	$\approx$70% 4π			$\Gamma=287$	

Table 1: The $L=1$ mesons shown with their widths and some decay fractions. The top part of the table shows the PDG assignments, while the bottom row shows this assignment for the scalar mesons.

from this is it is not possible to identify the $f_0(1500)$ as the f_0'. An identification as the first radial excitaion of the the $f_0(1370)$ also seems rather unlikely. The mass difference is to small, and the relatively narrow width of the $f_0(1500)$ make it improbable that it is a radial excitation. The obvious question is *What is the* $f_0(1500)$*?*.

θ	$\pi\pi$	$\eta\eta$	$\eta'\eta$	$K\bar{K}$
62°	3	0.2	1.7	14.2
118°	3	0.3	0.3	1.4
100°	3	0.15	0.5	3.5
$f_0(1500)$	3	0.70 ± 0.27	1.00 ± 0.46	≤ 0.36
Pure Glueball	3	1	0	4

Table 2: The expected decay fractions for the f_0' for three mixing angles. In addition, the measured values for the $f_0(1500)$ and a pure scalar glueball are given.

Lattice calculations predict that the lowest mass scalar glueball should have a mass around 1550 MeV. However, for a pure glueball, one expects the flavor blind decays rates as given in equation 1. These are clearly in disagreement with the measured values of the $f_0(1500)$. The $f_0(1500)$ is not a *pure* glueball. However, the $f_0(1500)$ sits more or less in the middle of the isoscalar members of the scalar nonet, $f_0(1370)$, and an expected $f_0'(\sim 1500-1800)$. It would be quite surprising if the $f_0(1500)$ were not mixed into the scalar nonet. Amsler and Close [17] argue that this is exactly what has occurred. In this paper, they are able to explain the decay pattern of the $f_0(1500)$ as a glueball mixed into the scalar nonet.

If the $f_0(1500)$ is the scalar glueball, then one would expect to see it in other production mechanisms. Both radiative J/Ψ decays and central production are expected to be gluon rich channels. Recent reanalysis of Mark III data [18] on $J/\Psi \rightarrow \gamma(\pi^+\pi^-\pi^+\pi^-)$ show evidence for a state at 1505 MeV/c^2 decaying to two S–wave di–pion systems, $(\sigma\sigma)$. In addition, recent analysis by the WA91 collaboration [19] on centrally produced $\pi^+\pi^-$ and $\pi^+\pi^-\pi^+\pi^-$ final states,

$$pp \rightarrow p_f(\pi^+\pi^-)p_s \ and\ pp \rightarrow p_f(\pi^+\pi^-\pi^+\pi^-)p_s$$

show evidence for the $f_0(1500)$. These data can be described as an interference between the $f_0(1370)$ and the $f_0(1500)$, with both resonances being observed in both the $\pi^+\pi^-$ and $\pi^+\pi^-\pi^+\pi^-$ final states. In addition, the GAMS experiment has observed a $J^{PC} = 0^{++}$ state decaying to $4\pi^\circ$, $\eta\eta$ and $\eta\eta'$ [16]. This centrally produced state is quoted with a mass of 1590, but may be the $f_0(1500)$.

Summary

There is currently good evidence that the scalar gluball has been observed. This object, the $f_0(1500)$ has a decay pattern which is most simply described as the scalar glueball mixed into the scalar nonet. In addition, it is observed in three different gluon rich production mechanisms. However, there are several missing measurements which are needed to clarify this. In particular, a measurement of $f_0(1500) \rightarrow \bar{K}K$ is quite important. In addition, the $f_0'(1500-1800)$ needs to be found. We hope to see both of these completed at LEAR in the next couple of years.

References

[1] E. Aker *et al.*, Nucl. Instrum. Methods A**321**, 69, (1992).

[2] S. U. Chung, *et al.*, submitted to **Z. Phys. C**, (1994).

[3] K. L. Au, D. Morgan and M. R. Pennington, Phys. Rev. D**35**, 1633, (1987).

[4] C. Amsler, *et al.*, **Coupled Channel Analysis of Antiproton Proton Annihilation into $\pi^\circ\pi^\circ\pi^\circ$, $\pi^\circ\eta\eta$ and $\pi^\circ\pi^\circ\eta$**. Accepted for publication in Phys. Lett. B., (1995).

[5] C. Amsler, *et al.*, Phys. Lett. B**342**, 433, (1995).

[6] V. V. Anisovich, *et al.*, Phys. Lett. B**323**, 233, (1994).

[7] C. Amelser *et al.*, **High Statistics Study of the $f_0(1500)$ decay into** $\eta\eta$. Accepted for publication in Phys. Lett. B, (1995).

[8] C. Amsler *et al.*, Phys. Lett. B**291**, 347, (1992).

[9] C. Amsler, *et al.*, Phys. Lett. B**333**, 277, (1994).

[10] M. Boutemeur and M. Poulet, Hadron 89, ed. F. Binon, J. M. Frère, J. P. Peigneux – (Ed. Frontiérs 1989), p.119.

[11] C. Amsler *et al.*, Phys. Lett B**340**, 259, (1994).

[12] L. Gray *et al.*, Phys. Rev. D**27**, 307, (1983).

[13] C. Amsler, *et al.*, Phys. Lett. B**322**, 431, (1994).

[14] K. Hikasa, *et al.*, Phys. Rev. D**50 II**, (1994).

[15] D. Aston *et al.*, Nucl. Phys. B**301**, 525, (1988).

[16] F. Binon *et al.*, Nuovo Cimento **78A**, 313, (1983), and **80A**, 303, (1984).

[17] C. Amsler, F. E. Close, Phys. Lett. B**353**, 385, (1995).

[18] D. V. Bugg, I. Scott, B. S. Zou, V. V. Anisovich, A. V. Sarantsev, T. H. Burnett, S. Sutlief, Phys. Lett. B**353**, 378, (1995).

[19] F. Antinori *et al.*, Phys. Lett. B**353**, 589, (1995).